

Schottky-barrier induced spin relaxation in spin injection

Y. Y. Wang and M. W. Wu*

*Hefei National Laboratory for Physical Sciences at Microscale,
University of Science and Technology of China, Hefei, Anhui, 230026, China and*

Department of Physics, University of Science and Technology of China, Hefei, Anhui, 230026, China[†]

(Dated: June 29, 2018)

An ensemble Monte Carlo method is used to study the spin injection through a ferromagnet-semiconductor junction where a Schottky barrier is formed. It is shown that the Schottky-barrier-induced electric field which is confined in the depletion region and is parallel to the injection direction, is very large. This electric field can induce an effective magnetic field due to the Rashba effect and cause strong spin relaxation.

PACS numbers: 72.25Dc, 72.25.Hg, 72.25Rb, 85.75-d

Spin injection from a ferromagnetic metal contact into a non-magnetic low-dimensional semiconductor structure is one of the prerequisites for the realization of the next generation high-speed low-power devices based on spin degree of freedom.^{1,2,3} Notwithstanding the fact that many efforts have been devoted to this problem experimentally,^{4,5} an efficient room-temperature spin injection is still far away from the horizon.⁵ In the meantime, there are many theoretical investigations^{7,8,9} on the spin injection through the ferromagnet-semiconductor junction where a high potential Schottky barrier is formed.⁶ In these studies the interface is treated through various boundary conditions.^{7,8} Large (up to 100 %) spin injections are reported in these theories. Very recently Shen *et al.* reported a first ensemble Monte Carlo (MC) simulation of the spin injection through a Schottky barrier into a semiconductor quantum well (QW).⁹ In this study, the Schottky barrier is treated carefully through the simulation. Still they reported a substantial spin polarization after the injection to a length scale in the order of 1 μm at room temperature without external magnetic field. Therefore there must be something missing in the theories in dealing with the ferromagnet-semiconductor junctions.

It is noted that the Schottky barrier induces a very large electric field parallel to the QW. Such an electric field can induce an effective magnetic field due to the Rashba effect¹⁰ and can therefore cause a strong reduction of the spin polarization after the injection. This effect has long been neglected in the literature. A quantitative estimation of this new relaxation mechanism requires an accurate computation of the electric field induced by the Schottky barrier which varies strongly with the position and is confined in the depletion region. For this purpose we apply an ensemble MC simulation to simulate the Schottky barrier and examine the spin relaxation induced by this additional relaxation mechanism under various conditions.

We study a ferromagnet-semiconductor diode which is one of the elements for many spintronic devices.¹¹ The spin-polarized particles are injected from a bulk ferro-

magnetic metal into a GaAs QW through a Schottky barrier by both thermionic emission and tunnelling injection, excluding the recombination in the space-charge region and the hole injection from the metal to the semiconductor.⁶ The direction of injection is parallel to the QW plane. The electron transport in the QW is based on the semiclassical approximation, simply including a “drift” and a “scattering” process: During the “drift” process, the spin is influenced by both the Rashba¹⁰ and the Dresselhaus¹² spin-orbit interactions. The method of the MC simulation has been laid out in detail in Ref. 13 for the Schottky barrier simulation, in Refs. 14,15 for the spin transport simulation and in Ref. 9 for the spin injection simulation. For the inhomogeneous electron distribution in the depletion region, the compression/expansion technique presented by Martin *et al.*¹⁶ has to be applied. In this report we do not repeat these details except the differences which are addressed in the following.

At finite temperature T , the total current injected from a ferromagnetic metal to a semiconductor through the Schottky barrier is written as⁶

$$j_{ms}(E_x) = \frac{A^*T}{k_B} \int_0^\infty T_{ms}(E_x) f_m(E) [1 - f_{sc}(E)] dE, \quad (1)$$

where k_B denotes the Boltzmann constant and A^* stands for the Richardson constant. $T_{ms}(E_x)$ is the tunnelling probability through the barrier at the energy E_x which represents the kinetic energy along the x -direction (the injection direction). It is 1 for $E_x \geq \Phi_B$ and $T_{ms}(E_x) = \exp\{-\frac{2}{\hbar} \int_0^{x_{tp}} \sqrt{2m^*[E_c(x) - E_x]}\}$ for $0 < E_x < \Phi_B$ following the WKB approximation. Φ_B represents the Schottky barrier height at the metal-semiconductor interface, x_{tp} is the electron position after tunnelling and $E_c(x)$ stands for the bottom of the conduction band in the semiconductor. $f_m(E)$ and $f_{sc}(E)$ are the electron distribution functions in the ferromagnetic metal and semiconductor separately with E standing for the total energy. It is emphasized here that unlike the previous works,^{9,13} the current and the tunnelling probability are only functions of E_x , instead of E . After injection, elec-

trons start travelling in the QW subject to the spin-orbit interactions, the electric field and the electron-phonon and possible electron-impurity scattering. The spin-orbit interaction is described by $H_{so}(x) = H_R(x) + H_D$, with the spacial variable-dependent Rashba term

$$H_R(x) = \gamma[(\sigma_x k_y - \sigma_y k_x)\mathcal{E}_z - k_y \sigma_z \mathcal{E}_x(x)] , \quad (2)$$

the linear Dresselhaus term $H_D^{(1)} = \beta(k_z^2)(\sigma_y k_y - \sigma_x k_x)$ and the cubic Dresselhaus term $H_D^{(3)} = \beta(\sigma_x k_x k_y^2 - \sigma_y k_y k_x^2)$. $\mathcal{E}_x(x)$ in Eq. (2) is the Schottky-barrier-induced electric field (SBIEF). The effective magnetic field induced by it in Eq. (2) has a significant influence to the spin relaxation and has long been overlooked in the literature.

We apply the MC method to study the spin injection from the magnetic Fe to (001) GaAs QW through a Schottky contact. The well width is 8 nm. The Schottky barrier height in the simulation is fixed to be $\Phi_B = 0.72$ eV.¹⁷ We use the following spin-orbit coupling constants: $\beta = 28$ eV·Å³ for the Dresselhaus effect¹⁸ and $\gamma = 740$ eV·Å² for the Rashba one.¹⁹ The channel length along the spin transport is $L_x = 2.5$ μm. The injection takes place at the Fe/GaAs interface at $x = 0$. As we investigate the spin injection from the source, the drain is assumed to be in Ohmic contact with the QW. In the figures of this paper, we only show the results for the initial 1 μm. In the MC simulation, we divide L_x into 500 cells and choose the time step to be $\Delta t = 1$ fs. To achieve the steady transport region, we run the simulation program for 10000 time steps and get the results by averaging over the last 3000 steps. The initial spin polarization is always assumed to be along the x -axis throughout this paper.

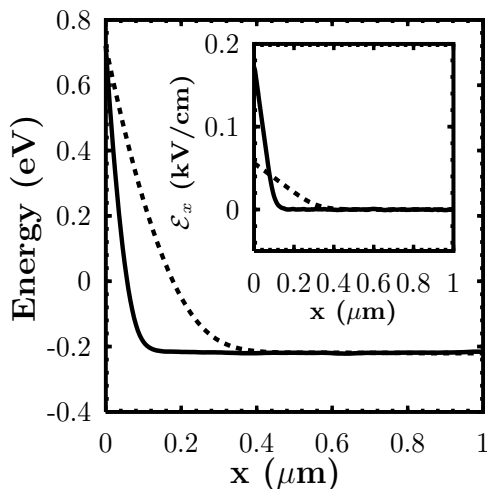


FIG. 1: Energy of the simulated Schottky barriers for two electron densities n at bias $V = 0.2$ V and $T = 300$ K. Solid curve: $n = 10^{11}$ cm⁻²; Dotted curve: $n = 10^{10}$ cm⁻². The corresponding electric fields are shown in the inset.

The simulated Schottky barrier shape, which is determined by the solution of the Poisson equation and

the MC simulation of the electron distributions self-consistently, is shown in Fig. 1 for different electron densities n in semiconductor QW. An inverse bias voltage $V = 0.2$ V is applied in the simulation, which is in favor of the electron injection from the ferromagnetic metal into the semiconductors.⁶ The large bending near the contact indicates the existence of a depletion layer where the electron concentration is negligible. It also gives an electric field $\mathcal{E}_x(x)$ which is shown in the inset of the figure. It can be seen that the Schottky barrier becomes thicker when the electron density in the QW is decreased. This is in consistent with the approximation relation that the Schottky barrier width is proportional to $n^{-1/2}$.⁶ Due to the change of the shape of the barriers, the SBIEF changes also at different electron densities as shown in the inset of Fig. 1.

Because of the large population of the spin-unpolarized electrons in the device, especially beyond the depletion region, the total spin polarization averaged over all the particles at a given position reduces to nearly zero at about $x = 20$ nm.^{9,20} We want to get the spin evolution of the injected electrons, so our simulation only get the spin polarization at each grid averaged over the injected spin-polarized electrons. In fact, the spin polarization of electrons in the interface of the ferromagnetic metal is determined by the spin-dependent density of states of electrons in the ferromagnetic contact. Nevertheless, in order to investigate spin polarization clearly, we assume the injected carrier is $S_x = 100$ % spin polarized first. We use $|S| = \sqrt{S_x^2 + S_y^2 + S_z^2}$ to denote the spin polarization of the injected electrons. Moreover, differing from the previous works^{9,15} where the electron density is as high as 10^{12} cm⁻², in the present work we only concentrate on the case with density being smaller than 10^{11} cm⁻². This is because that when the electron density is high, the chemical potential is large compared to $k_B T$. Therefore one should not use the Boltzmann distribution. Nevertheless, the MC method treats the scattering semiclassically and does not contain any distribution function. Consequently, it can only be applied to the problems with low electron density.

In Fig. 2 the spin polarization $|S|$ is plotted as function of the position x at temperatures $T = 300$ and 70 K without (the red and blue or the dashed and dotted curves) and with (the green and pink or the solid and chain curves) the SBIEF $\mathcal{E}_x(x)$ in the Rashba term [Eq. (2)]. The electron density is 10^{10} cm⁻² in the simulation. We also show the effects of the cubic Dresselhaus term to the spin relaxation by performing the simulation with (the blue and pink or the dotted and chain curves) and without (the red and green or the dashed and solid curves) $H_D^{(3)}$. It is seen from the figure that the SBIEF $\mathcal{E}_x(x)$ in Eq. (2) leads to a pronounced spin relaxation in the depletion region. The spin polarization is almost zero after the depletion layer, in contracts to the previous report of a substantial amount at the length scale of 1 μm.⁹ The spin relaxation in all the cases is due to the

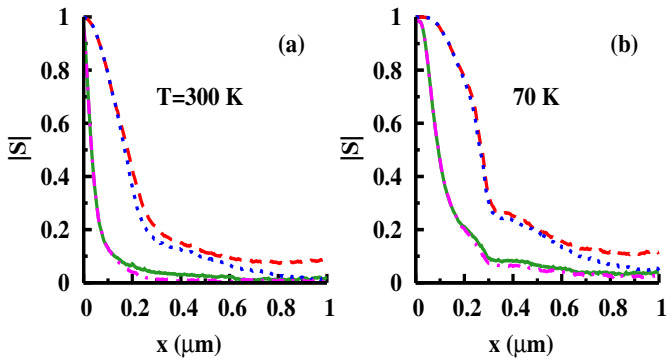


FIG. 2: (Color online) Spin polarization evolution at different temperatures without (the red and blue or the dashed and dotted curves) and with (the green and pink or the solid and chain curves) SBIEF $\mathcal{E}_x(x)$ in the Rashba term. The effect of the cubic Dresselhaus term is shown by including (the blue and pink or the dotted and chain curves) and excluding (the red and green or the dashed and solid curves) this term in the simulation. $n = 10^{10} \text{ cm}^{-2}$.

D'yakonov and Perel' mechanism.²¹ It is further noted from the figure that after the fast initial drop of the spin polarization in the depletion region, the spin polarization also slowly decreases with the position. This is because of the spin relaxation induced by the Rashba terms from the electric field perpendicular to the QW, *i.e.*, \mathcal{E}_z , and the Dresselhaus terms. This is in contrary to the results reported by Shen *et al.*,⁹ where they show that the spin polarization keeps almost constant beyond the depletion region. It is further seen from the figure that the third-order Dresselhaus term has marginal effect on the spin relaxation, especially at the depletion region where the Rashba term is dominant. This is because that the energy along the y direction ($k_B T$) is small, so that k_y^2 is small compared to k_z^2 in the Dresselhaus term.

We further investigate the effect of the SBIEF to the spin injection at higher electron density (but still barely in the non-degenerate regime). Curves in Fig. 3 are exactly corresponding to the cases in Fig. 2 except the electron density being 10^{11} cm^{-2} , an order of magnitude larger. It is seen from the figure that after the depletion region of Fig. 3, the injected spin polarizations all become smaller compared to the corresponding cases in Fig. 2. This is due to the enhanced Rashba and Dresselhaus terms at high electron densities. It is seen from the figure that the effective magnetic field induced by the SBIEF $\mathcal{E}_x(x)$ in Eq. (2) again markedly reduces the spin injections. It is further noted from the figure that the cubic Dresselhaus term $H_D^{(3)}$ shows larger influence than the low electron density case. This is because that the SBIEF is much larger at the high electron density case (see Fig. 1). This field drives electrons to a much larger $|k_x|$ and gives a larger cubic Dresselhaus term. It is also seen from Fig. 3 that the effect of cubic Dresselhaus term gradually reduces with the decrease of temperature. This

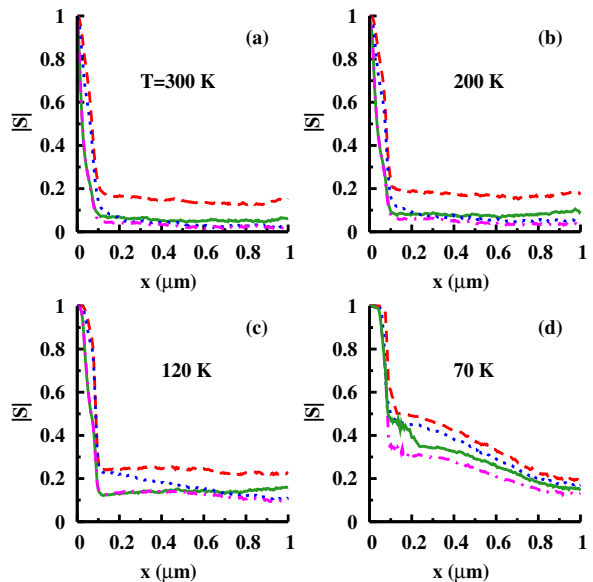


FIG. 3: (Color online) Same as Fig. 2 but with the electron density $n = 10^{11} \text{ cm}^{-2}$.

is because k_y^2 becomes smaller for lower temperature.

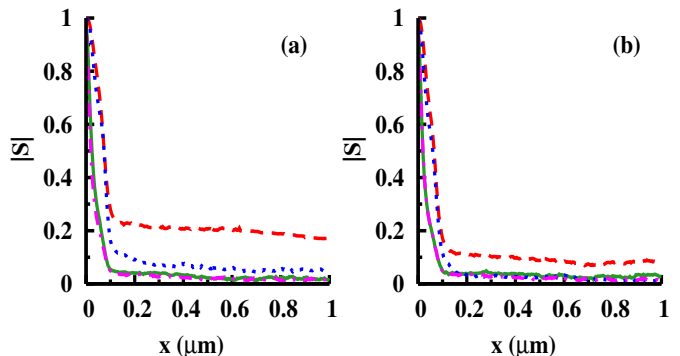


FIG. 4: (Color online) Comparison of the MC simulation with the Boltzmann sampling (a) and the Fermi sampling (b) for electrons at relatively high density $n = 10^{11} \text{ cm}^{-2}$. $T = 300 \text{ K}$. The meanings of the curves are all the same as those in Figs. 2 and 3.

It is noted that the MC method cannot be applied to the strong degenerate (high density) case as reported by Shen *et al.* where the electron density is taken as high as 10^{12} cm^{-2} .^{9,15} In the strong degenerate case, the electron distribution in the scattering cannot be overlooked any more and the MC method fails. Moreover, the Boltzmann sampling which is independent of the density, should be changed into Fermi sampling. In fact, even for the density at 10^{11} cm^{-2} , the non-degenerate approximation is already barely valid. In Fig. 4 we show the spin injections by using different samplings (Fig. 4(a) for Boltzmann sampling and Fig. 4(b) for Fermi sampling) at $n = 10^{11} \text{ cm}^{-2}$, with the scattering still kept to be

semiclassical. One can clearly find the marked difference. This is because when the Boltzmann sampling is used, the energy along the y -axis is fixed in the range of $k_B T$, regardless of the density. However, it is much larger by the Fermi sampling at high density case. Therefore, at high density case, the Rashba and the Dresselhaus terms are both weaker from the Boltzmann sampling. This leads to a larger spin polarizations. For density at 10^{10} cm^{-2} reported in Fig. 2, both samplings give the same results.

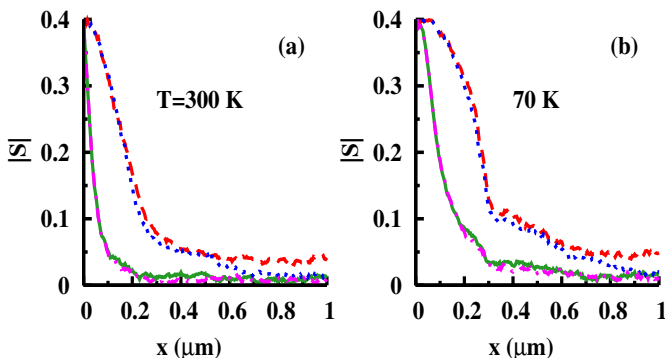


FIG. 5: (Color online) Same as Fig. 2 but with the initial spin polarization being 40 %.

In Figs. 2-4, we assume the injected electron spin polarization is 100 %. In fact, the initial spin injection, which is determined by the spin-state probability of electrons in the ferromagnetic contact and can be obtained from the microscopic models of ferromagnetic metal,²² is about 40 %. Figure 5 shows the results of the spin polarization inside the semiconductor QW with electron

density $n = 10^{10} \text{ cm}^{-2}$, when the initial injected electron spin polarization is 40 %. The main results are all the same as those shown in Fig. 2. As the initial spin polarization is low, the spin polarization beyond the depletion layer is lower than the corresponding case in Fig. 2 and reduces to zero more quickly.

In conclusion, an ensemble MC method is used to simulate the spin-polarized electron injection through a Schottky barrier and transport in 2D semiconductor QW with both Rashba and Dresselhaus spin-orbit coupling. We show that the SBIEF not only drives electron to a higher momentum states during the injection, which influences the spin relaxation via the Dresselhaus and the Rashba term, but also provides an effective magnetic field due to the Rashba effect. We show that this SBIEF-induced effective magnetic field is very strong and gives a pronounced effect to the spin dephasing at the Schottky barrier area. Consequently the spin injection becomes almost negligible after the Schottky barrier region. This effect has long been overlooked in the literature. Moreover, this effective magnetic field also provides additional relaxation due to the many-body effect²³ which is beyond the scope of the MC simulation and will be reported elsewhere.

This work was supported by the Natural Science Foundation of China under Grant Nos. 90303012 and 10247002, the Natural Science Foundation of Anhui Province under Grant No. 050460203 and SRFDP. We would like to thank S. T. Chui, M.-C. Cheng, L. Sun, M. Shen and S. Saikin for valuable discussions. One of the authors (MWW) would like to thank S. Zhang at University of Missouri Columbia for hospitality where this paper is finalized.

* Author to whom correspondence should be addressed; Electronic address: mwwu@ustc.edu.cn.

† Mailing Address.

¹ S. A. Wolf, *J. Supercond.* **13**, 195 (2000).

² *Semiconductor spintronics and quantum computation*, ed. by D. D. Awschalom, D. Loss, and N. Samarth (Springer-Verlag, Berlin, 2002).

³ I. Žutić, J. Fabian, and S. Das Sarma, *Rev. Mod. Phys.* **76**, 323 (2004).

⁴ A. T. Hanbicki, B. T. Jonker, G. Itskos, G. Kioseoglou, and A. Petrou, *Appl Phys. Lett.* **80**, 1240 (2002); V. F. Motsnyi, J. De Boeck, J. Das, W. Van Roy, G. Borghs, E. Goovaerts, V. I. Safarov, *ibid.* **81**, 265 (2002); A. T. Hanbicki, O. M. J. van't Erve, R. Magno, G. Kioseoglou, C. H. Li, and B. T. Jonker, *ibid.* **82**, 4092 (2003).

⁵ P. R. Hammer, B. R. Bennett, M. J. Yang, and M. Johnson, *Phys. Rev. Lett.* **83**, 203 (1999); H. J. Zhu, M. Ramsteiner, H. Kostial, M. Wassermeier, H. P. Schönherr, and K. H. Ploog, *ibid.* **87**, 016601 (2001); T. Manago and H. Akinaga, *Appl. Phys. Lett.* **81**, 694 (2002); H. Ohno, K. Yoh, K. Sueoka, K. Mukasa, A. Kawaharazuka, and M. E. Ramesteiner, *Jpn. J. Appl. Phys., Part 1* **42**, L1 (2003).

⁶ S. M. Sze, *Physics of Semiconductor Devices* (Wiley, New York, 1981).

⁷ M. Johnson and J. Byers, *Phys. Rev. B* **67**, 125112 (2003); G. Schmidt, D. Ferrand, L. W. Molenkamp, A. T. Filip, and B. J. van Wees, *Phys. Rev. B* **62**, R4790 (2000); E. I. Rashba, *ibid.* **62**, R16267 (2000); A. Fert and H. Jaffrès, *ibid.* **64**, 184420 (2001); J. D. Albrecht and D. L. Smith, *ibid.* **66**, 113303 (2002)

⁸ A. M. Bratkovsky and V. V. Osipov, *J. Appl. Phys.* **96**, 4525 (2004); V. V. Osipov and A. M. Bratkovsky, *Phys. Rev. B* **70**, 205312 (2004).

⁹ M. Shen, S. Saikin, and M.-C. Cheng, *J. Appl. Phys.* **96**, 4319 (2004).

¹⁰ Yu. Bychkov and E. I. Rashba, *J. Phys. C* **17**, 6039 (1984).

¹¹ S. Datta and B. Das, *Appl. Phys. Lett.* **56**, 665 (1990).

¹² G. Dresselhaus, *Phys. Rev.* **100**, 580 (1955).

¹³ L. Sun, X. Y. Liu, M. Liu, G. Du, and R. Q. Han, *Semicond. Sci. Technol.* **18**, 576 (2003).

¹⁴ A. Bournel, V. Delmouly, P. Dollfus, G. Tremblay, and P. Hesto, *Physica E* **10**, 86 (2001).

¹⁵ S. Saikin, M. Shen, M.-C. Cheng, and V. Privman, *J. Appl. Phys.* **94**, 1769 (2003); M. Shen, S. Saikin, M.-C. Cheng,

- and V. Privman, *Math. Comput. Simul.* **65**, 351 (2004).
- ¹⁶ M. J. Martín, T. Gonzalez, D. Pardo, and J. E. Velazquez, *Semicond. Sci. Technol.* **11**, 380 (1996).
- ¹⁷ J. R. Waldrop, *Appl. Phys. Lett.* **44**, 1002 (1984).
- ¹⁸ M. Cardona, N. E. Christensen, and G. Fasol, *Phys. Rev. B* **38**, 1806 (1988).
- ¹⁹ J. Nitta, T. Akazaki, and H. Takayanagi, *Phys. Rev. B* **38** 1806 (1988).
- ²⁰ J. D. Albrecht and D. L. Smith, *Phys. Rev. B* **68**, 035340 (2003).
- ²¹ M. I. D'yakonov and V. I. Perel', *Sov. Phys. JETP* **33**,1053 (1971).
- ²² W. H. Butler, X. G. Zhang, Xindong Wang, Jan Van EK, and J. M. MacLaren, *J. Appl. Phys.* **81**, 5518 (1997).
- ²³ M. W. Wu and C. Z. Ning, *Eur. Phys. J. B* **18**, 373 (2000); M. Q. Weng and M. W. Wu, *J. Appl. Phys.* **93**, 410 (2003); *Phys. Rev. B* **68**, 075312 (2003); M.Q. Weng, M.W. Wu, and L. Jiang, *ibid.* **69**, 245320 (2004).